Droplet evaporation of alcohol-biodiesel blends

Alexis Tanner and William Hallett*
Department of Mechanical Engineering, University of Ottawa
Ottawa, Ontario, K1N 6N5, Canada

Abstract

This work presents experimental data on the droplet evaporation of blends of biodiesel with 1-propanol and 1-pentanol and compares them to the results of numerical models of droplet evaporation. The phase equilibrium of the non-ideal mixture of alcohol with biodiesel was modelled using activity coefficients calculated from the UNIFAC method, which was shown to accurately reproduce experimental VLE data from the literature. Droplet evaporation experiments were performed for 1-propanol / biodiesel and 1-pentanol / biodiesel blends at temperatures of 450°C and 700°C. The numerical modelling compared two different liquid phase models: well-mixed and diffusion-limited. The diffusion-limited model was found to best represent the droplet evaporation process, particularly early in the droplet lifetime. Internal boiling and bubble formation were observed for all mixtures, driven by the large difference in boiling point between the components (around 200˚C). The diffusion-limited model was able to roughly predict the conditions under which bubble formation could occur.

Keywords: droplet evaporation; biodiesel; alcohol fuels; biodiesel/alcohol blends; continuous mixtures; alternative fuels

*Corresponding author. E-mail hallett@uottawa.ca, tel. 1-613-562-5800 ext. 6281

1. Introduction

The use of biodiesel in Diesel engines has increased over the years since biodiesel has lower net average greenhouse gas emissions than petroleum Diesel [1 - 3]. Alcohols, which can also be bio-based, can be added to biodiesel to improve engine performance as well to reduce engine emissions [4 - 8], and also to improve other biodiesel fuel properties, specifically the cloud point (CP), pour point (PP), and cold filter plugging point (CFPP) [7]. Work on alcohol/biodiesel blends initially focussed on methanol and ethanol, for which there is now a reasonably extensive literature. More recently attention has turned to higher alcohols such as butanol and pentanol [9 – 11], but for these there is much less information available, particularly with regards to the fundamental questions of droplet evaporation and phase equilibrium. The purpose of this paper is therefore to use experiments on droplet evaporation combined with numerical modelling to determine how droplet behaviour and vapour-liquid equilibrium may best be modelled for biodiesel blended with 1-propanol and 1-pentanol.

Most work on alcohol/biodiesel blends has been performed in engines [4 – 12], but there have also been a few studies on individual droplets. Botero *et al.* [13] burned free-falling ethanol-biodiesel droplets in a vertical furnace, while Pan and Chiu [14] studied suspended droplets of biodiesel with methanol, ethanol, and propanol under zero-gravity conditions. Hoxie *et al.* [15, 16] burned suspended droplets of butanol and pentanol blended with vegetable oil (not biodiesel). All these works deal with combustion of single droplets; however, in a spray flame, droplets do not as a rule burn individually, and it is droplet *evaporation* without combustion that is the more relevant process. Saha *et al.* [17] have studied droplet evaporation of biodiesel and of ethanol, but not blends thereof, and the droplet evaporation of blends with higher alcohols remains unexplored.

A consistent observation of combustion tests with alcohol/biodiesel blends has been the occurrence of “microexplosions”, most likely caused by volatile alcohol components at the center of the droplet suddenly vaporizing [14 – 16]. These observations have been made with blends of methanol, ethanol, and propanol with biodiesel, and a key factor here is that all these have a large difference between the boiling

points of the alcohol and biodiesel components. Microexplosions have been observed both with droplets supported on fibres [14 – 16] and for freely-falling ethanol/biodiesel droplets [13].

Since alcohols are polar molecules, they tend to form non-ideal mixtures, and consequently a number of papers have appeared on the phase equilibrium of blends of alcohol with biodiesel or fatty acid methyl esters (the main constituents of biodiesel) [18 - 23]. The available literature has so far confined itself to blends with methanol or ethanol, partly because much of the interest in phase equilibria centers on the production process for methyl- and ethyl-esters. For pure biodiesel, which is essentially non-polar, Raoult's law and simple vapour pressure equations such as the Antoine or the Clausius-Clapeyron have been used successfully [24, 25], but for alcohol mixtures it has proved necessary to use more complex descriptions of phase equilibrium such as the use of activity coefficients calculated using the UNIFAC or NRTL method [20], or cubic or other equations of state [21 - 23].

It is evident from this brief survey that there is little information on the droplet evaporation behaviour of blends of biodiesel with higher alcohols (*i.e.* C_3 or longer chains); hence the motivation for the present work, which will focus on 1-propanol and 1-pentanol blends with biodiesel.

2. Experiments

Droplet evaporation experiments were performed using the suspended droplet/moving furnace technique, with apparatus and instrumentation as described elsewhere [26, 27]. The droplet suspension was a 0.002" (0.05 mm) diameter bare wire Type K thermocouple equipped with a ~0.6 mm bead of refractory cement for the droplet to hang on. Detailed assessments of the influence of suspending fibres indicate that their effects should be negligible for wire this fine [26, 27]. A video camera was used to film the evaporation process, and droplet diameters were measured from frames taken at regular time intervals within the video. The droplets were generated with a microlitre syringe set to a volume of 2 μL, giving a droplet diameter of about 1.6 mm. An approximately prolate spheroidal shape under the influence of gravity was assumed, and the diameter was defined as the volume equivalent diameter of this shape, determined by measuring major

and minor diameters. The entire apparatus was enclosed and supplied with a nitrogen atmosphere to ensure that only evaporation occurred, not combustion.

Experiments were performed on blends of 1-propanol / biodiesel and 1-pentanol / biodiesel with alcohol concentrations of 5%, 10%, 15%, and 20% by volume at furnace temperatures of 450°C and 700°C. (The equivalent mass fractions were 4.57%, 9.17%, 13.82%, and 18.52% for the 1-propanol / biodiesel blend and 4.63%, 9.29%, 13.99%, and 18.73% for 1-pentanol / biodiesel blend.) The biodiesel was a sample of commercial product supplied by Innoltek, Saint-Jean-sur-Richelieu, Québec, while the 1-propanol and 1- pentanol were Sigma-Aldrich products with purities of ≥ 99.9% and ≥ 99.0% respectively.

3. Numerical Modelling

3.1 Continuous Thermodynamics

The numerical models used in this work represent fuels using continuous thermodynamics, which describes a mixture of discrete components as a continuous distribution function $f(I)$ [28, 29] with mean θ and standard deviation σ. Multiple distribution functions, each with its own parameters, can be used to represent different chemical families in the mixture. Apart from computational efficiency, the advantage of using continuous thermodynamics rather than modelling each individual component is that it allows an accurate model of a mixture to be set up using a distillation curve, without the need for a detailed chemical analysis.

In this work a gamma distribution function is used with the distribution origin set to zero, and the component molecular weight is the distribution variable I. Each pure alcohol is described with a very narrow distribution having θ equal to the molecular mass and a σ of 2 kg/kmol. The biodiesel is assumed to comprise several different fatty acid methyl esters (FAME) and a small quantity of unconverted monoglycerides (MGC), and it was accordingly represented by two different distribution functions, one for each of these chemical families. The parameters for these were determined from a distillation test combined with a continuous mixture numerical simulation of this test [27], as shown in Figure 1. The test was conducted according to ASTM D86-20 [30], except that water instead of an ice bath was used for cooling, and the test

was done at atmospheric pressure rather than under vacuum, since no coking of the sample occurred. Table 1 gives the fitted distribution parameters. As is typical for biodiesel, most of the fuel boiled in a narrow temperature range of 345 - 380°C, indicating the presence of a small number of different FAME's, with a brief final rise to higher temperatures as the MGC fraction evaporated.

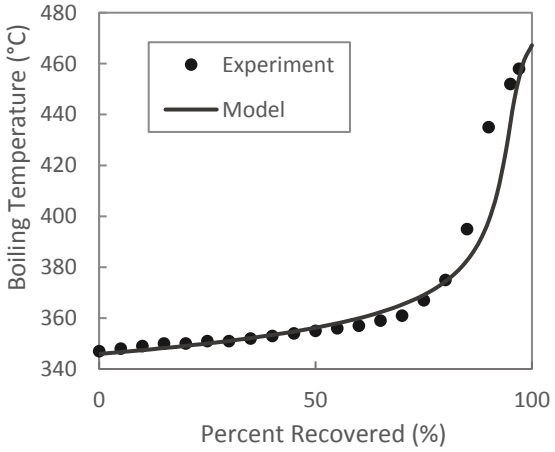

Figure 1: Distillation curve for biodiesel and distillation model using two continuous mixtures as defined in Table 1

Table 1: Composition of biodiesel as two continuous mixtures.

Component	Mass Fraction (mass %)	Distribution Mean Molecular Weight θ (kg/kmol)	Standard Deviation σ (kg/k1mol)
Fatty Acid Methyl Esters	93	322	26
Monoglycerides	7	470	10

3.2 Vapour-Liquid Equilibrium Model

An appropriate method must be chosen to describe the non-ideal vapour-liquid equilibrium (VLE) of the mixtures. An effective approach for mixtures of alcohols is to introduce an activity coefficient γ_i to correct Raoult's law:

$$P_i = \gamma_i x_i P_{vpi} \quad (1)$$

In earlier work on ethanol / fuel oil blends [27], excellent results were attained by using the multicomponent Wilson equation for γ_i, with the parameters fitted using activity coefficients at infinite dilution calculated using the SPACE correlation [31]. Unfortunately, the parameters for the SPACE equations were not available for some of the functional groups in FAME's and MGC's; neither were relevant experimental VLE data to be found. The choice therefore fell on the UNIFAC method [31], which allows VLE prediction without the need for experimental data. UNIFAC calculates the activity coefficient using a combinational term and a residual term [31]:

$$\ln \gamma_i = \ln \gamma_i^C + \ln \gamma_i^R \quad (2)$$

Table 2 and Table 3 lists the values of the parameters used in the UNIFAC calculations for the functional groups present in FAME's, MGC's and alcohols

Component vapour pressures for use in eq. (1) were calculated using a continuous mixture formulation of the Clausius-Clapeyron equation fitted for each individual component distribution [28, 29].

Table 2: UNIFAC functional group volume and area parameters [31, 32]

Functional Subgroup (k)	Functional Main Group	W_k	U_k
CH_3	CH_2	0.9011	0.848
CH_2	CH_2	0.6744	0.540
CH	CH_2	0.4469	0.228
CH=CH	C=C	1.1167	0.867
OH	OH	1.0000	1.200
CH_2COO	CCOO	1.6764	1.420

Table 3: UNIFAC functional group interaction parameters a_{mn} in Kelvins [31,32]

n / m	CH_2	C=C	OH	CCOO
CH_2	0	86.02	986.5	232.1
C=C	-35.36	0	524.1	37.85
OH	156.4	457.0	0	101.1
CCOO	114.8	132.1	245.4	0

Biodiesel is a multi-component fuel, containing several different FAMEs and MGCs. However, the UNIFAC method uses a single molecule in its calculations, and therefore a representative molecule needs to be chosen to represent the biodiesel mixture. A representative molecule is selected by first generating an approximate composition for the biodiesel as individual components. The composition was selected such that four FAME molecules represent the FAME fuel fraction; one FAME for the lower molecular weight portions of the fuel, one for the higher, and two for the intermediate molecular weights. Previous work by Hallett and Legault [25] has shown that FAME components with double bonds exhibit essentially identical behaviour to saturated FAME components during the distillation and droplet evaporation processes [25]. The present work therefore uses saturated FAME's, except that one double-bonded FAME is selected to represent the fact that most biodiesels do include some unsaturated species. The resulting composition comprises three saturated FAME's (*n*-paraffin chains C18, C20, C22), one C20 FAME with a single double bond, and one MGC. The mass fraction of each component was then determined by fitting a discrete component distillation model to the experimental distillation data as shown in Figure 2. The resulting estimated composition of the biodiesel is shown in Table 4.

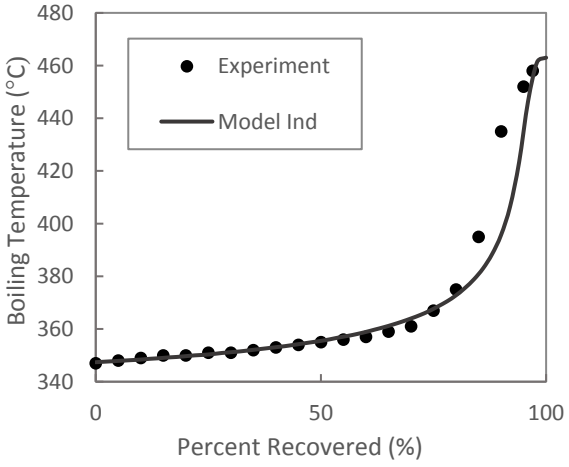

Figure 2: Distillation curve for biodiesel and distillation model using individual components as defined in Table 4

Table 4: Estimated composition of biodiesel as individual components

FAME or MGC Component	Mass Fraction	Molecular Weight (g/mol)
Methyl Stearate (C18)	0.36	298.5
Methyl Arachidate (C20)	0.17	326.6
Methyl 11(Z)-Eicosenoate (C20)	0.12	324.5
Methyl Behenate (C22)	0.28	354.6
Glycerol 1-Monohexacosanoate	0.07	470.8

There are 4 FAMEs present in this assumed composition and a representative FAME molecule needs to be selected to represent the FAME fraction in UNIFAC calculations. There are four different ways to select a representative species: as the lowest molecular weight FAME, the highest molecular weight, the mass average FAME or the mole average FAME. Depending on the selected method, the number of functional groups present in the representative molecule varies, as shown in Table 5.

Table 5: Number $N_k^{(i)}$ of each functional group k required using different choices for the representative component of the FAME mixture i,

Representative FAME species choice	$N_k^{(i)}$			
	CH_3	CH_2	CH_2COO	CH=CH
Lowest Molecular Weight	2	15	1	0
Highest Molecular Weight	2	19	1	0
Mol Average	2	16.4552	1	0.1281
Mass Average	2	16.57	1	0.1290

These different methods were compared by calculating the VLE of a continuous FAME mixture with propanol and comparing this with the VLE of the discrete component FAME mixture with propanol, as shown in Figure 3. The selection of the representative molecule can be seen to have no significant effect on the calculated VLE, showing that non-ideal interactions between individual FAME components are insignificant. Therefore, only the non-ideal interactions between a FAME molecule and an alcohol molecule will influence the VLE of the mixture. This work therefore uses the mole average species as the representative compound for UNIFAC calculations for the FAME fraction. The presence or absence of

double bonds in the hydrocarbon chain of the representative FAME has a negligible effect on the VLE, and therefore a paraffinic chain was assumed. For the MGC fraction, the compound glycerol 1-monohexacosanoate listed in Table 4 was selected as the representative species.

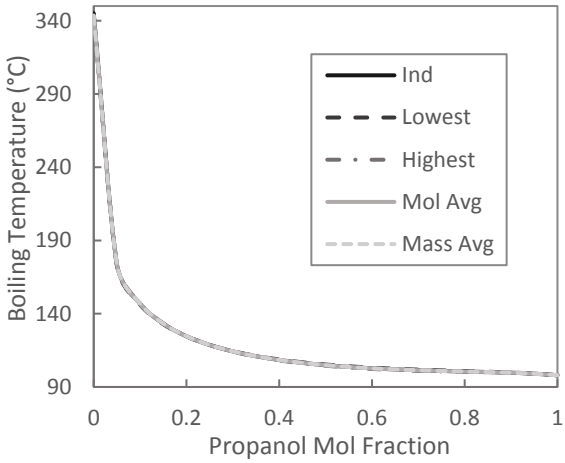

Figure 3: Vapour liquid equilibria of FAME mixture with propanol in which the FAME mixture is represented as individual components ("Ind") or as a continuous mixture with the functional groups represented by the molecule with the lowest molecular weight, highest molecular weight, mol average or mass average

Verification of the VLE calculation was done by comparing its results to experimental VLE data for individual FAME's with ethanol from the literature [21], as shown in Figure 4. The UNIFAC method agrees well with the experimental data points, whereas Raoult's law (shown for comparison) does not, illustrating the degree to which this mixture is non-ideal. One of these compounds (methyl oleate) contains one double bond, but this does not appear to affect the accuracy of the method save for one point at a FAME mol fraction of 0.9.

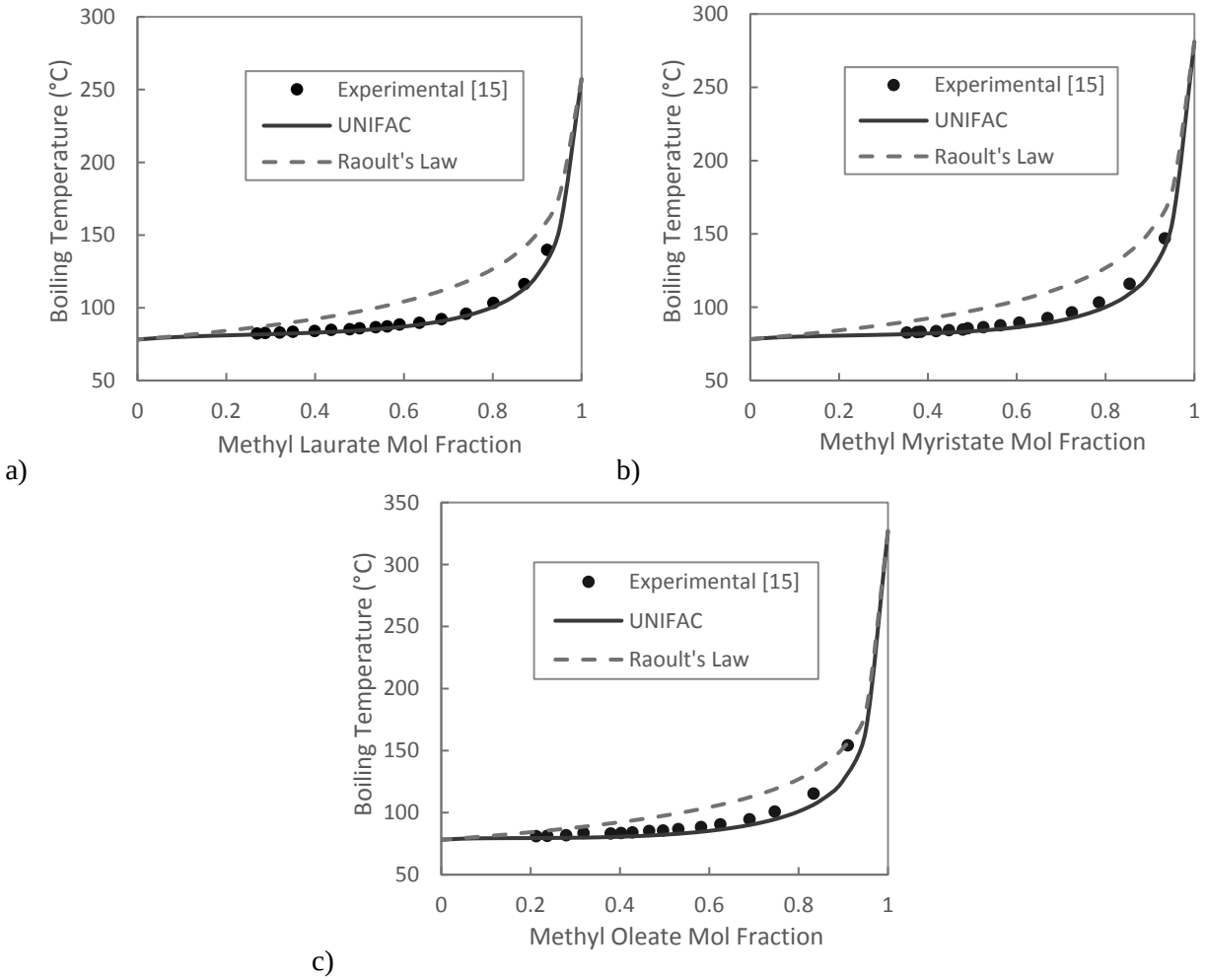

Figure 4: Comparison of vapour-liquid equilibria modelling using the UNIFAC method and Raoult's Law with experimental data [21]] for a) methyl laurate-ethanol, b) methyl myristate-ethanol, and c) methyl oleate-ethanol.

Calculations were also compared to experimental VLE data for biodiesel-ethanol [18 – 20], as shown in Figure 5. The biodiesel parameters of the present work (Table 1) were used for the calculations, as the published biodiesel boiling temperatures agreed closely with those of Figure 1, and there was some uncertainty as to the biodiesel compositions used in the references. The UNIFAC method agrees well with the experimental data, except for two data points from da Silva *et al*. [19], possibly attributable to differences in biodiesel composition.

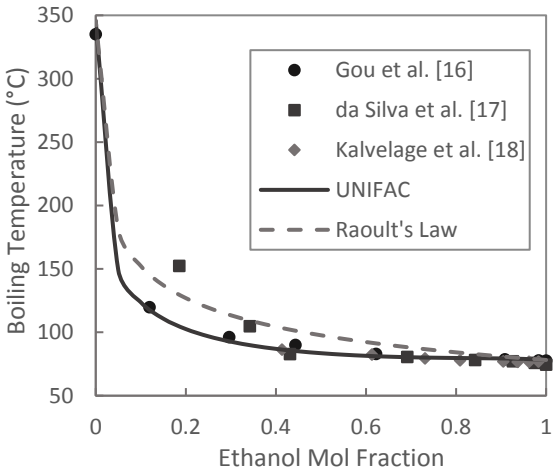

Figure 5: Comparison of vapour-liquid equilibrium modelling using the UNIFAC method and Raoult's Law with experimental data for biodiesel-ethanol [16–18].

3.3 Droplet Evaporation Models

Two different numerical models were used to calculate droplet evaporation. Both assume spherical symmetry, and both are based on a continuous thermodynamics treatment of mixture properties, with the same properties correlations used for both.

The first model assumes that the liquid phase is well-mixed (*i.e.* of uniform composition and temperature), and the vapour phase quasi-steady, so that analytical solutions result for the vapour phase coupled with a numerical solution for droplet heating. Full details are given in earlier work [33, 27]. Natural convection was included using a standard heat transfer correlation and the heat/mass transfer analogy as described elsewhere [29]. For this model, the mixture was represented by the full three distribution functions: two for the biodiesel (Table 1) and one for the alcohol.

The second model uses a diffusion-limited liquid phase, so that concentrations of the component distributions change radially within the liquid phase of the droplet and any changes in local liquid composition result solely from liquid diffusion. In reality, there is some fluid motion and mixing within the droplet, and this is accounted for by multiplying the liquid diffusivity by a mixing factor χ, which is typically between 2 - 4 [34, 35]. In this work, $\chi = 3$ is used, based on comparisons between experimental and calculated droplet temperature histories. However, the temperature inside the droplet is assumed uniform, since

thermal diffusivities in liquids are much larger than mass diffusivities. The diffusion-limited model computes a complete transient solution of both liquid and vapour phases using continuous thermodynamics to represent properties in both phases. Details are given in reference 34. Natural convection is dealt with by setting the outer boundary of the vapour phase calculation domain to a finite value δ corresponding to the boundary layer thickness in the film theory of mass and heat transfer [36]:

$$\frac{1}{\delta} = \frac{1}{R}\left(\frac{Nu_0}{2} - 1\right) \tag{3}$$

where R is the droplet radius and Nu_0 is the Nusselt number for free convection as determined from the correlation used for the well-mixed model [29]. The diffusion-limited model can only deal with two distribution functions, so that the biodiesel was represented by the FAME distribution alone (*i.e.* without the MGC fraction) for these calculations.

The use of continuous thermodynamics requires correlations for properties such as boiling point, enthalpy of vaporization, specific heat, density, thermal conductivity, and diffusivity as functions of temperature and species molecular mass. A separate set of correlations is needed for each distribution function. For the biodiesel constituents (FAME, MGC), the correlating equations and their parameters are given by Hallett and Legault [25]; the FAME component was assumed to be saturated. For the alcohols, the correlating equations are the same, and the parameters were fitted using standard correlations**Error! Reference source not found.**. Vapour phase properties for both models were evaluated at a reference state of (2/3 surface conditions + 1/3 ambient conditions) as prescribed by Hubbard *et al*. [33]. The liquid diffusivity for both alcohol and FAME fractions was calculated using a correlation for *n*- paraffins given in reference 34.

4. Results

The results for the biodiesel / 20% propanol mixture at 450°C show the characteristic observed behaviours of alcohol-biodiesel blends. Figure 6 compares the experimental droplet temperature and diameter with the models. The diffusion-limited model agrees well with experimental data; the exception

is the slight rise followed by a sudden fall in measured diameter during the second half of the droplet lifetime, which will be shown later to be due to bubble formation. The well-mixed model does not agree as well: in particular, it shows the droplet temperature flattening at 2 seconds and the droplet diameter decreasing to a line below the experimental data.

Both models include thermal expansion of the liquid, which is also evident in the measurements early in the droplet lifetime. The inclusion of natural convection contributes substantially to the success of the models: without it, predicted droplet lifetimes become substantially longer than measured. The sharp rise in measured temperatures near the end can be ignored: it occurs because the thermocouple bead becomes directly exposed to the furnace as the liquid disappears.

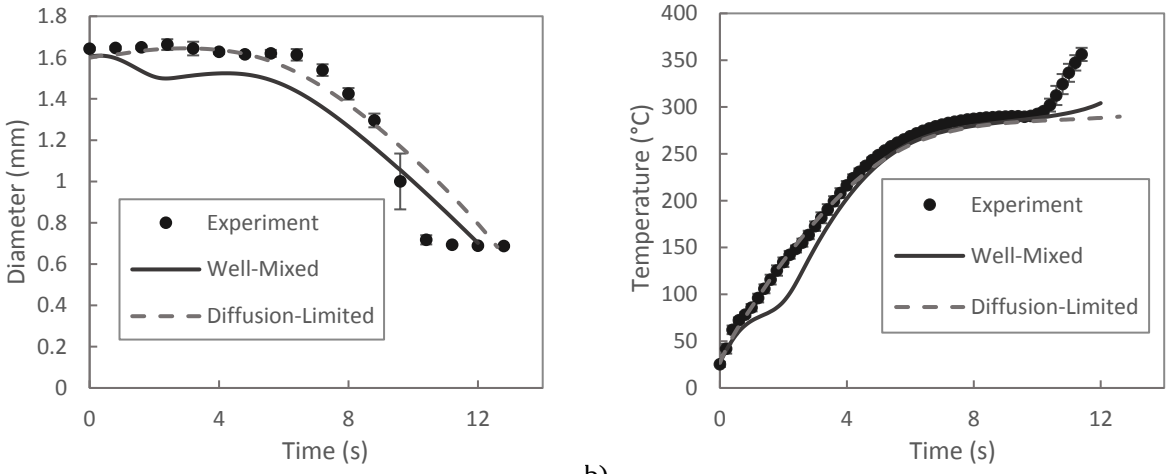

a) b)

Figure 6: a) Droplet diameter and b) droplet temperature for biodiesel with 20% propanol at 450°C. Points are averages and error bars are standard deviations of 8 individual measurements.

Figure 7 shows why the well-mixed model behaves differently from the diffusion-limited one by graphing the history of the vapour molar flux and vapour mol fraction at the surface for both models. Since propanol has a much lower boiling point than the biodiesel components, all the propanol in the well-mixed droplet evaporates early in the droplet lifetime as shown in Figure 7a). This causes a high molar flux of evaporating components G, which consumes more heat for vaporization; this reduces the available heat for droplet heating, making the temperature rise pause a little below the boiling point of propanol (Figure 6b). However, for the diffusion-limited model, the propanol has to slowly diffuse to the surface of the droplet

before evaporating, causing a smaller vapour flux and a more constant rate of droplet heating, as seen in Figure 6b). These results show that the diffusion-limited model best represents the data, and the same conclusion was reached for all other mixtures, including the pentanol ones. The slow transport of components within the liquid phase by diffusion is clearly essential to correctly modelling the process.

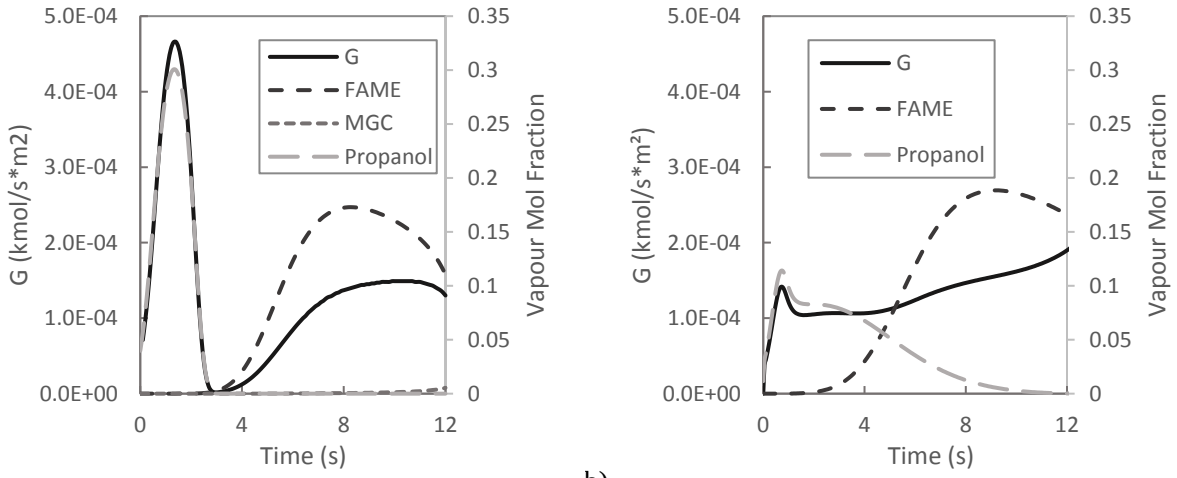

Figure 7: Calculated vapour molar flux and vapour mol fractions of a) well-mixed or b) diffusion-limited droplet for biodiesel with 20% propanol at 450°C.

The cause of the sudden drop in measured diameters in Figure 6a) is the formation of bubbles, as can be seen in the droplet photos in Figure 8.

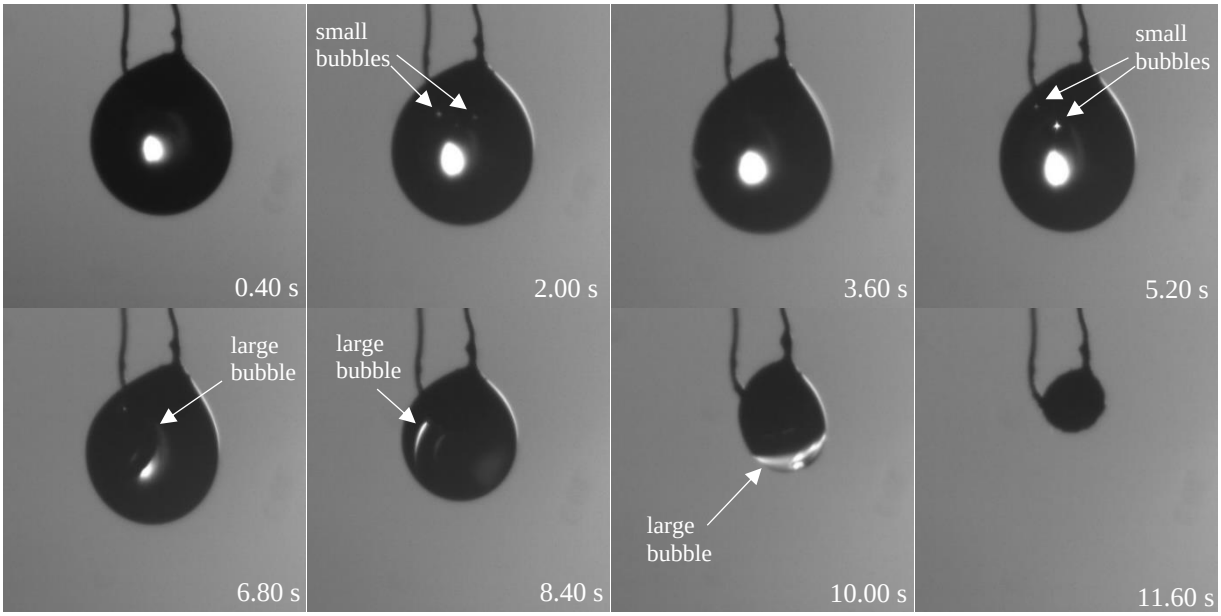

Figure 8: Droplet photos of biodiesel with 20% propanol during droplet evaporation at 450°C

Small bubbles appear as small specks of light at 2.00 and 5.20 seconds, while photos at 6.80, 8.40, and 10.00 seconds show a large bubble forming. The timing of the large bubble corresponds with the increase in experimental droplet diameter shown in Figure 6a) and its collapse with the sudden drop after 10 s.

After multiple droplet evaporation tests, a picture of the stages of droplet evaporation emerged as sketched in Figure 9. Initially, evaporation only occurs at the surface of the droplet (Figure 9a). As the droplet temperature continues to increase, eventually it will become greater than the boiling temperature within the droplet, and boiling and bubbling will start to occur, with the cement bead that the droplet hangs on acting as a nucleation site, as shown in Figure 9b). A further increase in droplet temperature causes more bubbles to form (Figure 9c) and then group together to form a large bubble (Figure 9d). The interior surface of the large bubble will act as a second surface where evaporation can occur, causing the large bubble to grow. Eventually the large bubble will occupy much of the droplet's volume (Figure 9e) and will break through the liquid layer to escape to the environment. The remaining liquid will then evaporate as a normal droplet as shown in Figure 9f).

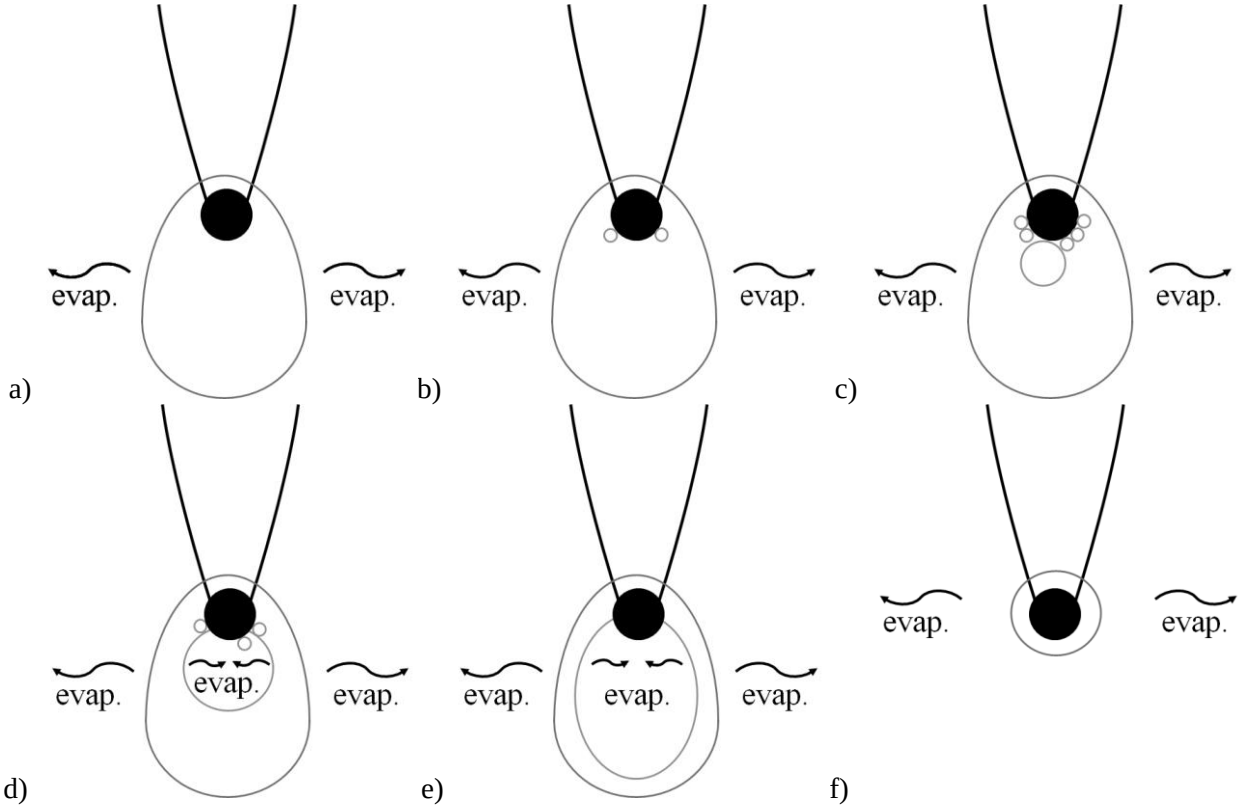

Figure 9: Stages of bubbling during droplet evaporation.

To show the effect of bubble formation on the experimental diameters, the volume of the large bubbles as estimated from photos was subtracted from the droplet's volume to get a new equivalent droplet diameter, shown as "Adjusted Experiment" in Figure 10. This corrected droplet diameter agrees well with the diffusion-limited model between 5.6 and 8.8 seconds. However, the experimental diameter still shows a sudden drop after 8.8 seconds. This corresponds to the large bubble escaping the droplet, indicating that some mass is ejected at this point. These observations show that the diffusion-limited model would agree well with experimental results if bubbling didn't occur. In real-life spray combustion, there is no droplet support, and thus no nucleation site for bubbles present. In that case, internal boiling would only occur if the limit of superheat was exceeded. Therefore, the diffusion-limited model should accurately represent the droplet evaporation process of alcohol-biodiesel blends in real-life spray applications.

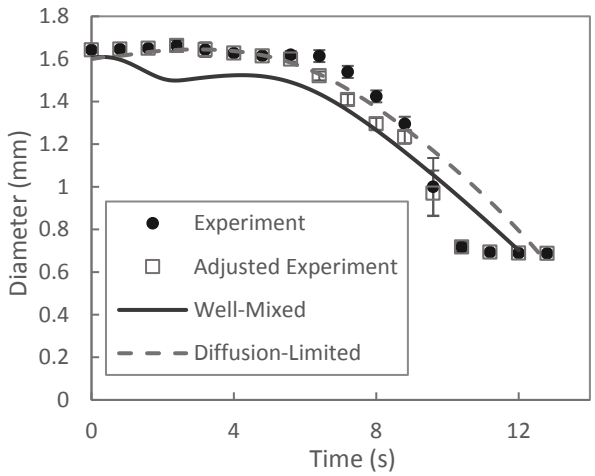

Figure 10: Droplet diameter versus time, showing the effect of deducting the internal bubble volume ("adjusted experiment") for biodiesel with 20% propanol at 450°C

The bubbling behaviour is a result of the slow pace of liquid phase diffusion, which causes significant quantities of volatile species (*i.e.,* alcohol) to remain at the droplet centre while the surface layer is depleted of these components. The ensuing radial concentration variations result in changes in liquid bubble point with position and time, as shown in Figure 11. The local bubble point is calculated from the concentration of liquid components at that radial position as predicted by the diffusion-limited model, and the figure shows that it lies below the droplet temperature starting from about 1.6 seconds and continuing for most of the droplet's lifetime. However, the bubble point at the surface always remains greater than the droplet's temperature because of the depletion of volatile components here. Internal boiling and bubbling can therefore occur throughout much of the droplet lifetime as long as there is a nucleation site, such as the cement bead, present. This behaviour, variously described as bubbling, "puffing" or "microexplosion", has become a familiar phenomenon whenever there is a large difference between component boiling points: it has been observed in combustion of blends of biodiesel with ethanol [13, 14], of soybean oil with butanol and pentanol [15, 16], of light alcohols with hydrocarbons [37, 38], and of water/oil emulsions [39, 40]. These works all deal with burning droplets, but bubbling can also occur in pure evaporation, despite the lower heat fluxes [27].

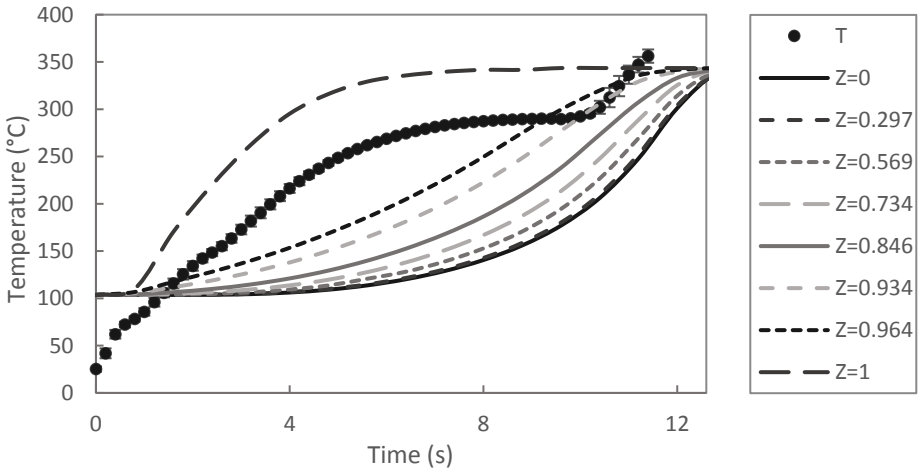

Figure 11: Measured droplet temperature (points) and calculated bubble point temperatures at different radial positions (Z = r/R) as a function of time for biodiesel with 20% propanol at 450°C.

Other trends were observed during the experimentation. For example, when performing droplet evaporation experiments at a furnace temperature of 700°C, bubbling was more vigorous (the frequency of bubble formation rose, the formation of large bubbles increased). This can be seen in the variation in experimental data points shown in Figure 12, where the experimental diameter can be seen to decrease briefly just after the first second. This is caused by vigorous bubbling which caused a few very small droplets to be ejected from the main droplet. The second decrease in experimental droplet diameter is caused by the formation and escape of the large bubble from the droplet.

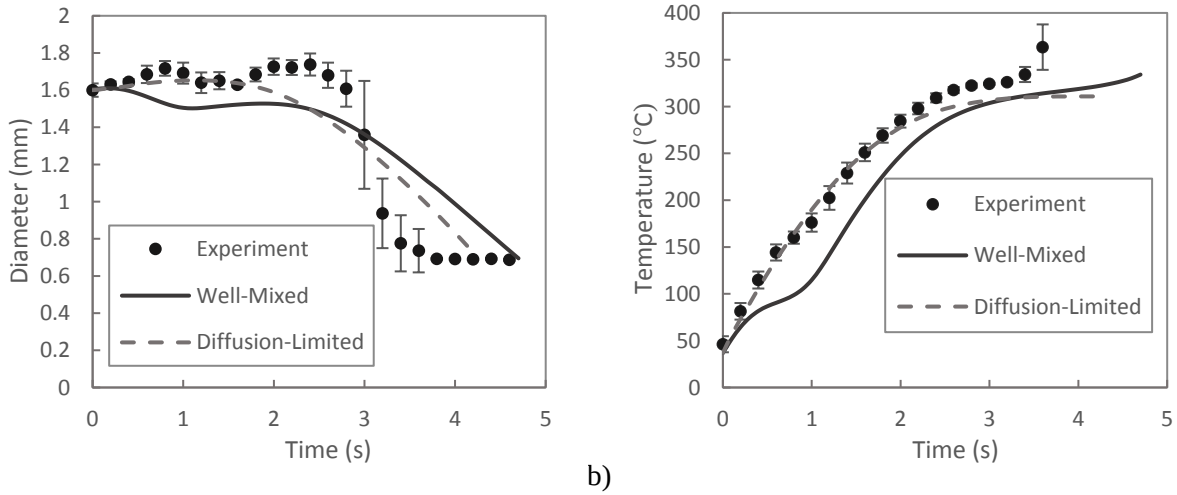

a) b)

Figure 12: a) Droplet diameter and b) droplet temperature for biodiesel with 20% propanol at 700°C

At low concentrations of the alcohol component, the well-mixed model results approach those of the diffusion-limited model (Figure 13), since at low concentrations the alcohol component has less influence on the vaporization rate. Boiling is still observed at low alcohol concentrations, but fewer bubbles form throughout the droplet lifetime. Large bubbles do form during droplet evaporation of biodiesel with a low alcohol concentration, but they do not reach the size of the whole droplet and thus do not greatly affect the experimental droplet diameter. This suggests that the well-mixed model could be used for low alcohol concentrations (below 5%). However, at alcohol concentrations of 10%, the difference between the well-mixed and diffusion-limited models is more noticeable, and thus the diffusion-limited model should be used to represent droplet evaporation when alcohol concentrations are greater than 5%.

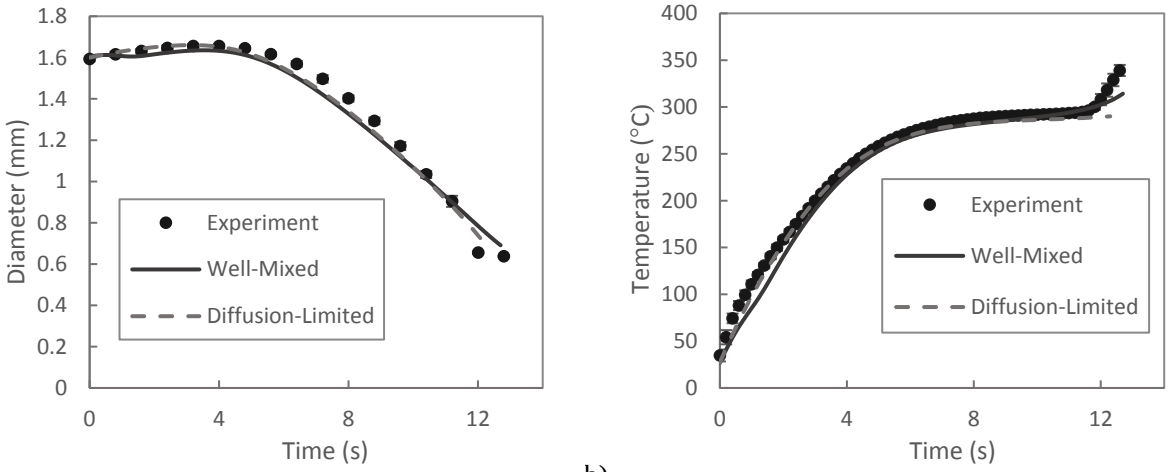

a) b)

Figure 13: a) Droplet diameter and b) droplet temperature for biodiesel with 5% propanol at 450°C

Experiments on droplets of 1-pentanol / biodiesel blends showed similar behaviour to that for propanol mixtures, with some minor differences. Figure 14 summarizes results for 20% pentanol. Comparing with the 20% propanol blend (Figure 6), there is less difference between the two models, mainly because the boiling point difference between the alcohol and the biodiesel has been reduced from about 240˚C for propanol to 200˚C. This suggests that blends with higher alcohols could be adequately modelled with a well-mixed model. The smaller boiling point difference also reduced the range of conditions for

which bubbling could occur, and the bubbling was weaker. Because of this, the deviations of the data from the model during bubbling are smaller (Figure 14).

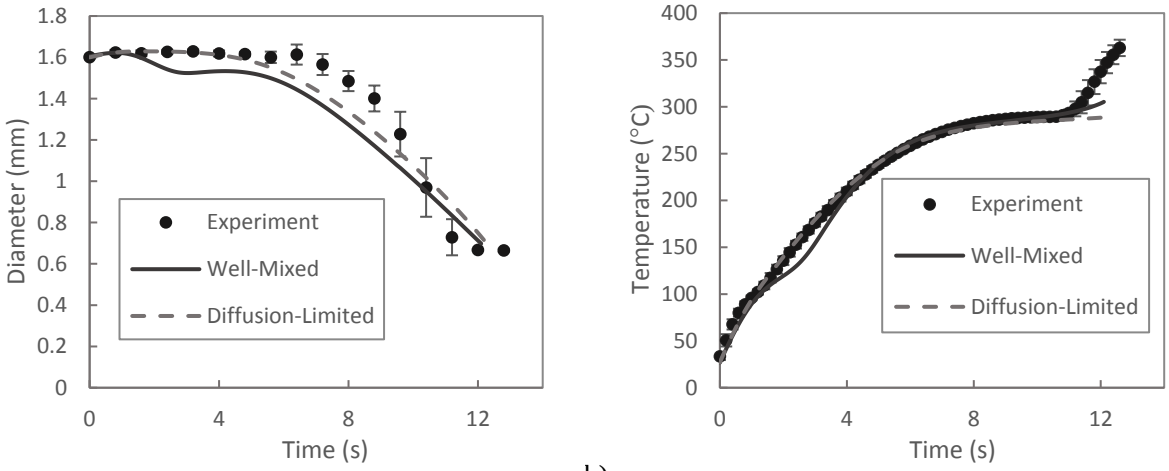

a) b)

Figure 14: a) Droplet diameter and b) droplet temperature for biodiesel with 20% pentanol at 450°C

Figure 15 shows evaporation for biodiesel with 5% pentanol. Due to the low alcohol concentration, the well-mixed and diffusion-limited models produced very similar results, and as with 5% propanol, the well-mixed model could be used here. Bubbling was observed, including the formation of a large bubble, which causes the experimental droplet diameters to be larger than the models' (Figure 15a).

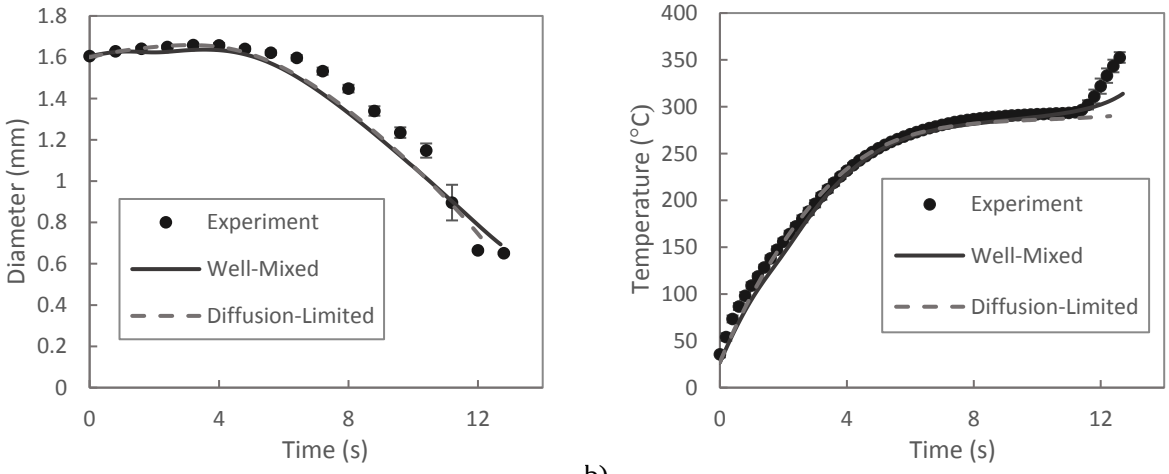

a) b)

Figure 15: a) Droplet diameter and b) droplet temperature for biodiesel with 5% pentanol at 450°C

5. Conclusion

This paper has presented experimental data and numerical model results for the evaporation of mixtures of alcohols (1-propanol, 1-pentanol) and biodiesel. Comparisons with published experimental vapour-liquid equilibria of common FAME's and of biodiesel with ethanol show that activity coefficients calculated from the UNIFAC method can accurately represent the phase equilibrium of these blends, whereas Raoult's law is inadequate for this purpose. Because of the large difference in boiling points between the alcohols and the FAME's, a droplet evaporation model which includes the calculation of liquid phase diffusion is necessary to accurately represent the evaporation of these blends, although a well-mixed liquid model may also yield reasonable results at low alcohol concentrations (< 5%) or for longer chain alcohols. Internal boiling and bubble formation were observed, caused by the volatile alcohol remaining at the center of the droplet as the droplet heats. This was encouraged by the presence of the droplet suspension thermocouple in the experiments; this acted as a nucleation site for bubble formation, which therefore may not necessarily occur for free droplets.

Acknowledgements

This work was supported by the Natural Sciences and Engineering Research Council under Discovery Grant RGPIN/001650-2011 to W. Hallett. The authors are grateful to Innoltek, Saint-Jean-sur-Richelieu, Québec, for providing the biodiesel sample.

Nomenclature

FAME fatty acid methyl ester

G molar flux, kmol/m^2 s

MGC monoglyceride

P_i partial pressure of component i

P_{VPi} saturation pressure of component i

x_i mol fraction of component i

γ_i activity coefficient of component i

θ distribution function mean, kg/kmol

σ distribution function standard deviation, kg/kmol

χ mixing factor multiplying the liquid diffusity

References

[1] Knothe, G.; Razon, LF. Biodiesel fuels. *Prog. Energy Combust. Sci*. **2017**, 58, 36–59.

[2] Koh, LP.; Ghazoul, J. Biofuels, biodiversity, and people: Understanding the conflicts and finding opportunities. *Biological Conservation* **2008**, 141, 2450–2460.

[3] Knothe, G.; Krahl, J.; Gerpen, J. *The Biodiesel Handbook*, 2nd ed., Urbana, Illinois: Academic Press and AOCS Press, 2010.

[4] Kumar, S.; Cho, J.H.; Park, J.; Moon, I. Advances in diesel–alcohol blends and their effects on the performance and emissions of diesel engines. *Renewable Sustainable Energy Rev.* **2013,** 22, 46–72.

[5] Yilmaz, N.; Sanchez, T. M. Analysis of operating a diesel engine on biodiesel-ethanol and biodiesel-methanol blends. *Energy* **2012**, 46, 126-129.

[6] Yilmaz, N. Performance and emission characteristics of a diesel engine fuelled with biodiesel-ethanol and biodiesel-methanol blends at elevated air temperatures. *Fuel* **2012**, 94, 440-443.

[7] Torres-Jimenez, E.; Svoljšak-Jerman, M.; Gregorc, A.; Lisec, I.; Dorado, M. P.; Kegl, B. Physical and Chemical Properties of Ethanol−Biodiesel Blends for Diesel Engines. *Energy Fuels* **2010**, 24, 2002–2009.

[8] Tse, H.; Leung, C.W.; Cheung, C.S. Investigation on the combustion characteristics and particulate emissions from a diesel engine fueled with diesel-biodiesel-ethanol blends. *Energy* **2015**, 83, 343-350.

[9] Rathinam, S.; Balan, K. N.; Subbiah, G.; Sajin, J. B.; Devarajan, Y. Emission study of a diesel engine fueled with higher alcohol-biodiesel blended fuels. *Int. J. Green Energy* **2019**, 16, 667-673.

[10] Yilmaz, N.; Vigil, F. M.; Davis, S. M.; Calva, A. Effect of biodiesel-butanol fuel blends on emissions and performance characteristics of a diesel engine. *Fuel* **2014,** 135, 46-50.

[11] Yilmaz, N.; Sanchez, T. M. Analysis of operating a diesel engine on biodiesel-ethanol and biodiesel-methanol blends. *Energy* **2012**, 46, 126-129.

[12] Aydin, H.; Ilkilic, C. Effect of ethanol blending with biodiesel on engine performance and exhaust emissions in a CI engine. *Applied Thermal Engineering* **2010**, 30, 1199-1204.

[13] Botero, M. L.; Huang, Y.; Zhu, D. L.; Molina, A.; Law, C.K. Synergistic combustion of droplets of ethanol, diesel and biodiesel mixtures. *Fuel* **2012**, 94, 342-347.

[14] Pan, K-L.; Chiu, M-C. Droplet combustion of blended fuels with alcohol and biodiesel/diesel in microgravity condition. *Fuel* **2013**, 113, 757–765.

[15] Hoxie, A.; Schoo, R.; Braden, J. Microexplosive combustion behavior of blended soybean oil and butanol droplets. *Fuel* **2014**, 120, 22–29.

[16] Coughlin, B.; Hoxie, A. Combustion characteristics of ternary fuel Blends: Pentanol, butanol and vegetable oil. *Fuel* **2017**, 196, 488-496.

[17] Saha, A.; Kumar, R.; Basu, S. Infrared thermography and numerical study of vaporization characteristics of pure and blended bio-fuel droplets. *Int. J. Heat and Mass Transfer* **2010**, 53, 3862-3873.

[18] Guo, Y.; Zhong, J.; Xing, Y.; Li, D.; Lin, R. Volatility of Blended Fuel of Biodiesel and Ethanol. *Energy Fuels* **2007**, 21, 1188–1192.

[19] da Silva, D.I.S.; Mafra, M.R.; da Silva, F.R.; Ndiaye, P.M.; Ramos, L.P.; Cardozo Filho, L.; Corazza, M.L. Liquid–liquid and vapor–liquid equilibrium data for biodiesel reaction–separation systems. *Fuel* **2013**, 108, 269–276.

[20] Kalvelage, P.M.S.; Albuquerque, A.A.; Barros, A.A.C.; Bertoli, S.L. (Vapor + Liquid) Equilibrium for Mixtures Ethanol + Biodiesel from Soybean Oil and Frying Oil. *Int. J. Thermodynamics* **2017**, 20, 159–164.

[21] Oliveira, M.B.; Miguel, S.I.; Queimada, A.J.; Coutinho, J.A.P. Phase Equilibria of Ester + Alcohol Systems and Their Description with the Cubic-Plus-Association Equation of State. *Ind. Eng. Chem. Research* **2010**, 49, 3452–3458.

[22] Oliveira, M.B.; Llovell, F.; Cruz, M.; Vega, L.F.; Coutinho, J.A.P. Phase equilibria description of biodiesels with water and alcohols for the optimal design of the production and purification process. *Fuel* **2014**, 129, 116-126.

[23] Xu, J.; Yan, T.; Yang, C.; Wang, Y.; Fang, T. Phase equilibrium thermodynamic modelling for the methanol + fatty acid methyl ester systems at high temperatures and pressures. *J. Biobased Materials and Bioenergy* **2016**, 10, 1-10.

[24] Rose, A.; Supina, W.R. Vapor pressure and vapor-liquid equilibrium data for methyl esters of the common saturated normal fatty acids. *J. Chemical and Engineering Data* **1961**, 6, 173-179.

[25] Hallett, W.L.H.; Legault, N.V. Modelling biodiesel droplet evaporation using continuous thermodynamics. *Fuel* **2011**, 90, 1221–1228.

[26] Sabourin, S.W.; Boteler, C.I.; Hallett, W.L.H. Droplet ignition of approximately continuous liquid mixtures of *n*-paraffins and *n*-alkyl aromatics. *Combust. Flame* **2016**, 163, 326-336.

[27] Hallett, W.L.H.; Beauchamp-Kiss, S. Evaporation of single droplets of ethanol-fuel oil mixtures. *Fuel* **2010,** 89, 2496-2504.

[28] Tamim, J.; Hallett, W.L.H. A continuous thermodynamics model for multicomponent droplet vaporization. *Chem. Eng. Science* **1995**, 50, 2933–2942.

[29] Hallett, W.L.H. A simple model for the vaporization of droplets with large numbers of components. *Combust. Flame* **2000**, 121, 334–344.

[30] American Society for Testing and Materials. ASTM D86-20: Standard Test Method for Distillation of Petroleum Products and Liquid Fuels at Atmospheric Pressure. ASTM International 2020.

[31] Poling, B.E.; Prausnitz, J.M.; O'Connell, J.P. *The Properties of Gases and Liquids*. 5th ed. New York: McGraw-Hill; 2001.

[32] DDBST GmbH, Dortmund Data Bank, www.ddbst.de (accessed December 31, 2020).

[33] Hubbard, G.L.; Denny, V.E.; Mills, A.F. Droplet evaporation: effects of transients and variable properties. *Int. J. Heat Mass Transfer* **1975**, 18, 1003-1008.

[34] Abdel-Qader, Z.; Hallett, W.L.H. The role of liquid mixing in evaporation of complex multicomponent mixtures: modelling using continuous thermodynamics. *Chem. Eng. Science* **2005**, 60, 1629–1640.

[35] Talley, D.G.; Yao, S.C. A semi-empirical approach to thermal and composition transients inside vaporizing fuel droplets. 21st Symposium (International) on Combustion **1988**, 609–16.

[36] Bird, R.B.; Stewart, W.E.; Lightfoot, E.N. *Transport Phenomena*. Wiley, New York, 1960.

[37] Lasheras, J.C.; Fernandez-Pello, A.C.; Dryer, F.L. On the disruptive burning of free droplets of alcohol/*n*-paraffin solutions and emulsions. 18th Symposium (International) on Combustion, **1980**, 293-305.

[38] Wang, C.H.; Lui, X.Q.; Law, C.K. Combustion and microexplosion of freely falling multicomponent droplets. *Combust. Flame* **1984**, 56, 175-197.

[39] Law, C.K. Internal boiling and superheating in vaporizing multicomponent droplets. *AIChE J.* **1978**, 24, 626-632.

[40] Lasheras, J.C.; Fernandez-Pello, A.C.; Dryer, F.L. Initial observations on the free droplet combustion characteristics of water-in-fuel emulsions. *Combust. Science and Technology* **1979**, 21, 1 – 14.

[41] Hallett, W.L.H.; Clark, N.A. A model for the evaporation of biomass pyrolysis oil droplets. *Fuel* **2006**, 85, 532-544.